

High-Magnesian Calcite:

Leaching of Magnesium in the Deep Sea

Abstract. *The high-magnesian calcite fraction of a shallow-water carbonate sand was converted to low-magnesian calcite after transport to the deep sea; strontium was also leached from the carbonate. Oxygen isotopic ratios indicate that loss of magnesium and strontium took place during recrystallization of the carbonate in the deep sea; this process did not alter textures of skeletal fragments. Previously, high-magnesian calcite was thought only to dissolve in the deep sea.*

Those marine organisms which utilize CaCO_3 for skeletal material build structures of aragonite, or low-magnesian calcite (<4 mole percent MgCO_3), or high-magnesian calcite (>4 mole percent MgCO_3). Upon the death of the organisms, the skeletal remains are incorporated in the sediments, where, in a shallow marine environment, they may persist indefinitely (1). Occasionally, turbidity currents or similar agents transport the remains to the deep sea where one or more of the calcareous phases are unstable.

The behavior of high-magnesian calcite under deep-sea conditions is poorly understood. At great depths, it is absent; whether it is dissolved out of the sediments or is selectively leached of magnesium to become low-Mg calcite was unknown, although Friedman (2), finding no progressive decrease in the magnesium content of high-Mg calcite with depth, favored dissolution. Similarly, Chave (3) showed that the fine carbonate fraction of pelagic sediments becomes enriched in low-Mg calcite by selective dissolution of both aragonite and high-Mg calcite. In contrast, we

here present data indicating that high-Mg calcite, deposited in the deep sea by turbidity currents, loses magnesium while the physical integrity, including structural and cellular features, of skeletal fragments is maintained.

We studied a coarse sand layer, 143 cm thick, found in a piston core obtained in the South Pacific from below 4230 m of water (4). The sand layer is graded and is notably lacking in fine material. Some fragments at the base of the layer have diameters up to 1 cm. Rapid transport and deposition are evidenced by the sharp boundary between the white sand and the brown, zeolitic, fine sediment beneath. There is a gradual transition upward from the top of the layer into more than a meter of the zeolitic sediment, the common pelagic deposit in this region of the South Pacific (5). Presently accepted sedimentation rates in this area (6) allow us to estimate that deposition of the sand layer occurred between one and a few million years ago.

Although fragments of basaltic rocks and minerals are also present in the sand layer, the bulk of the material

consists of carbonate skeletal fragments. Even though effects of both solution and physical abuse have degraded many of the carbonate grains beyond recognition, a sufficient number of identifiable fragments remain to indicate a shallow-water origin for the sand. These include alcyonarian spicules, echinoid spines, many disjointed segments of the calcareous red alga *Corallineae* (7), and numerous individuals of *Amphistegina madagascariensis*, a shallow-water, benthic foraminifer. We interpret the assemblage as having originated in a lagoonal or forereef environment, at depths probably not exceeding 30 m and at temperatures consistent with a tropical habitat. A probable source is the volcanic island of Anaa, located 67 km north of the core location; turbidity currents must have transported the sand to the deep sea (8).

Shallow-water organic carbonate sediments are predominantly aragonite and high-Mg calcite, a reflection of the skeletal composition of their invertebrate and algal progenitors. Although they were surely present initially, we detected neither aragonite nor high-Mg calcite by x-ray powder diffraction studies of the sand, nor did we find any aragonitic organisms (for example, madreporian corals, most pelecypods, and gastropods) by microscopic observation. The lack of aragonite is probably due to the fact that this phase readily dissolves under deep-sea conditions (2).

The absence of a high-Mg calcite peak in the diffraction pattern coupled

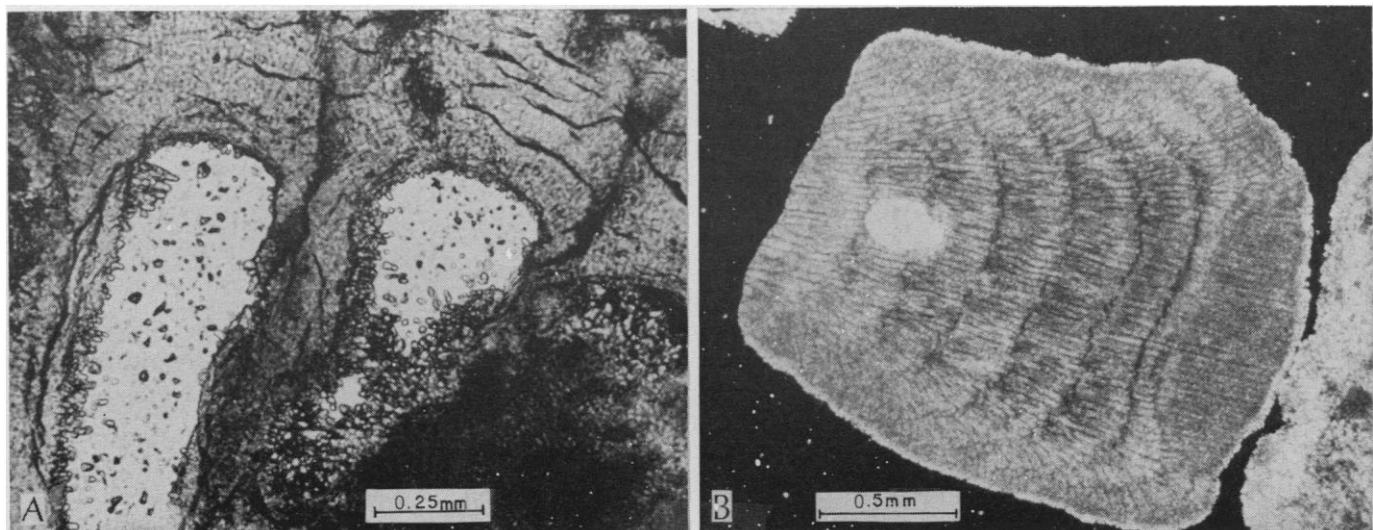


Fig. 1. Fragments from the deep-sea sand showing recrystallization without textural destruction. (A) Chambers of *Amphistegina madagascariensis*, with calcite crystals partially filling void spaces. (B) Segment of *Corallineae*, probably *Jania*, surrounded on three sides by small calcite crystals. The void spaces have been filled with sparry calcite but the cellular structure is well preserved.

Table 1. Comparison of $MgCO_3$ and $SrCO_3$ content and oxygen isotopic ratios of deep-sea core and reference samples. Values are calculated on the assumption that $CaCO_3 + MgCO_3 + SrCO_3 = 100$. The δO^{18} data are relative to the Chicago standard Pee-Dee belemnite No. 1. The first entries in the temperature column are calculated from δO^{18} values; numbers in parentheses are approximate surface temperatures (16). Calcium, magnesium, and strontium were determined by atomic absorption spectrometry after dissolution of the samples in acetic acid. Error in the determination is less than 3 percent.

Sample	Location	$MgCO_3$ (mole %)	$SrCO_3$ (mole %)	δO^{18}	Temperature (°C)
<i>Amphistegina</i> sp.	Cape Verde Is.	4.27		-1.69	24.2(24)
<i>A. madagascariensis</i> *	Kapingamarangi	7			(28)
<i>A. madagascariensis</i>	Oahu	6.29	0.183	-2.71	29.2(23)
<i>A. madagascariensis</i>	Amph 44 core	2.70	.059	+2.54	6.5(25)
Bulk sample	Amph 44 core	2.81	.045	+2.00	8.5(25)
Corallineae	Amph 44 core	3.01	.039	+1.95	8.6(25)
<i>Amphiroa</i>	Oahu	17.2	.119	-1.03	21.1(23)
<i>Corallina</i> †	California	12.9	.24		
<i>Jania</i>	Bermuda	17.8		-2.11	26.1(23)

* From Blackmon and Todd (9). † From Goldsmith *et al.* (17).

with an abundance of known high-Mg calcite organisms in the sand prompted us to look more closely at its chemical composition. The results, together with analyses of reference samples for comparison, are given in Table 1. Samples of *A. madagascariensis* and Corallineae (Fig. 1), hand-picked from the sand layer, contain, respectively, 2.70 and 3.01 mole percent $MgCO_3$, whereas a bulk sample of the sand contains 2.81 mole percent $MgCO_3$. Blackmon and Todd (9) report 7 mole percent $MgCO_3$ for *A. madagascariensis* from Bikini and Kapingamarangi atolls, and we find 6.29 mole percent $MgCO_3$ for the same species picked from beach sand from Oahu, although Atlantic species have been reported which contain as little as 3 mole percent $MgCO_3$ (9). Representative analyses of the three possible genera of Corallineae present in the deep-sea sand are also shown in Table 1. All are considerably higher in $MgCO_3$ than the Corallineae from the sand layer of core Amph 44. The analytical results show that magnesium has been lost from the Corallineae of the deep-sea sand and strongly indicate a removal of magnesium from both *A. madagascariensis* and the sand as a whole.

Further proof that chemical alteration has occurred is given by the low abundance of strontium in the deep-sea samples. This is best seen in terms of the ratio of atoms of $Sr \times 10^3$ to atoms of Ca. This ratio is about 0.5 in the deep-sea samples and 1.5 to 2 in the littoral specimens. A value of 4 has been found for foraminiferal $CaCO_3$ (10) and 3.4 to 9 for coralline algae. Only recrystallized fossils and limestones commonly have ratios less than 1.0, a result of the fact that replace-

ment and recrystallization lower the ratio of Sr to Ca (11).

The leaching of magnesium and strontium could have taken place either in the deep sea or through the action of meteoric water during some emergent, pretransport stage in the history of the sample; in fact, sea-level changes occurring during the Pleistocene could have contributed to subaerial exposure of the sand, as could the tectonic activity of Anaa, for which there is some evidence (12). In order to discriminate between these two possibilities we made use of the fact that the ratio of O^{18} to O^{16} of biogenic and sedimentary carbonates generally is a reflection of the environment in which they crystallize (13). The ratio remains unchanged if the carbonates are exposed to waters with different oxygen isotopic ratios or different temperatures unless recrystallization takes place, in which case the carbonates will assume a ratio reflective of the isotopic ratio and temperature of the water in which recrystallization has occurred (14). Thus, if the transformation of high-Mg calcite into the low-Mg phase occurred in the deep-sea sand through a process of microrecrystallization as suggested on the basis of microscopic examination of the material (Fig. 1), measurements of the ratio of O^{18} to O^{16} should give indications as to the environment of such transformation.

Accordingly, we determined the isotopic ratios in specimens of the deep-sea carbonate sand and in reference samples (Table 1). The δO^{18} values (relative to the Chicago standard Pee-Dee belemnite No. 1) of the reference *Amphistegina* and Corallineae range between -1.0 and -2.7 which, if we assume equilibration with standard sea-

water, correspond to water temperatures of 21° to 29°C. These temperatures are close to those of the water in which the organisms in question live. The original δO^{18} values of Corallineae and *Amphistegina* from the sand layer must have been close to those of the reference samples, yet the present measured values are between +1.9 and +2.5. These values indicate that (i) recrystallization did take place, without altering, however, the texture of the skeletal fragments, as shown in Fig. 1; (ii) the loss of Mg and Sr did not take place in meteoric water because in such a case the δO^{18} of the calcites would have become lower than the original values (15). Recrystallization and loss of Mg and Sr must have taken place in seawater. The calculated isotopic temperatures (6.5° to 8.6°C) are close to bottom temperatures at the core location (1° to 4°C); this suggests that isotopic readjustment occurred in the deep sea. We conclude that high-Mg calcite is converted gradually into low-Mg calcite under deep-sea conditions by a process of microrecrystallization; the loss of magnesium is paralleled by a depletion of strontium.

DAVID N. GOMBERG

ENRICO BONATTI

University of Miami, Rosenstiel School of Marine and Atmospheric Sciences, Miami, Florida 33149

References and Notes

1. R. A. Berner, *Amer. J. Sci.* **264**, 1 (1966).
2. G. M. Friedman, *Bull. Geol. Soc. Amer.* **76**, 1191 (1965).
3. K. E. Chave, *Limnol. Oceanogr.* **7**, 218 (1962).
4. The core in question (Amph 44) was recovered at 18°05'S, 145°41'W during the Amphitrite Expedition of the Scripps Institution of Oceanography. The length of the core is 457 cm. The carbonate sand layer extends from 38 to 181 cm from the top of the core. The accompanying gravity core, which appears to have stopped at the sand layer, contains 140 cm of zeolitic sediment.
5. E. Bonatti, *Trans. N.Y. Acad. Sci.* **25**, 938 (1963).
6. E. D. Goldberg and M. Koide, *Science* **128**, 1003 (1958).
7. One or more of the genera *Amphiroa*, *Corallina*, and *Jania* almost certainly comprise the algal component, although we were unable to make positive identification beyond the subfamily Corallineae (articulate coralline algae). Thus all three genera are represented for comparison in Table 1.
8. D. N. Gomberg, in preparation.
9. P. D. Blackmon and R. Todd, *J. Paleontol.* **33**, 1 (1959).
10. P. J. Wangersky and O. Joensuu, *J. Geol.* **72**, 477 (1964).
11. H. T. Odum, *Publ. Inst. Mar. Sci. Univ. Tex.* **4**, 38 (1957).
12. M. S. Doty, *Proc. Pacific Sci. Congr. Pacific Sci. Ass. 9th Bangkok, 1957* **4**, 148 (1962).
13. S. Epstein, R. Buchsbaum, H. Lowenstam, H. C. Urey, *Bull. Geol. Soc. Amer.* **62**, 1315 (1953).
14. C. E. Emiliani, *J. Geol.* **64**, 281 (1956); J. D. Milliman, *Science* **153**, 994 (1966).
15. S. Epstein and T. Mayeda, *Geochim. Cosmochim. Acta* **4**, 213 (1953); M. G. Gross and J. I. Tracey, Jr., *Science* **151**, 1082 (1966).

16. G. Dietrich, *General Oceanography* (Wiley, New York, 1963), chart 3.
 17. J. R. Goldsmith, D. L. Graf, O. I. Joensuu, *Geochim. Cosmochim. Acta* 7, 212 (1955).
 18. We thank the late Miss P. Morway, to whom we dedicate this work, for help with the isotopic analyses; M. Doty of the University of Hawaii and C. Emiliani for valuable discussions; S. Valdez for the strontium and

magnesium determinations; J. Andrews of the University of Hawaii for supplying some samples. Supported by NSF grant GA-1602 and ONR contract NONR 4008 (02). Contribution No. 1208 from the Rosenstiel School of Marine and Atmospheric Sciences, University of Miami.

12 January 1970; revised 16 April 1970 ■

Interstellar Scattering of Pulsar Radiation and Its Effect on the Spectrum of NP0532

Abstract. *Angular scattering in the interstellar medium results in multipath dispersion which can amount to more than one pulse period for pulsars of short period and high dispersion measure. The dispersion, if operative, imposes on the pulsation flux a cutoff inversely proportional to the fourth power of the observing wavelength. The low-frequency pulse shape of pulsar NP0532 suggests that this pulsar is subject to such scattering and that the observed low-frequency cutoff in the apparent spectrum is not an intrinsic property of the pulsar. In fact, there is evidence that NP0532 may be identified as the compact, low-frequency source in the Crab Nebula and that the pulsar may radiate in accordance with its high-frequency spectrum down to frequencies as low as 10 megahertz, although the periodic time variations are suppressed by the scattering below 100 megahertz.*

The time and frequency structure of the intensity fluctuations of pulsars is evidence for diffraction arising from irregularities in the density of free electrons in the interstellar medium (1-3). Important confirmation of the scintillation mechanism has been provided by recent observations of highly correlated intensity fluctuations over a long base line with time delays appropriate for a diffraction pattern traveling at a few tens of kilometers per second (4).

If one analyzes the intensity scintillations, it is possible to deduce the scale of the angular scattering associated with the diffraction (2, 3). The angular scattering will, in turn, give rise to single frequency temporal dispersion as a result of multipath propagation. If the temporal dispersion amounts to more than the pulsar period, the pulsation flux will appear to be reduced; the scattering mechanism transfers pulsation flux into continuous flux (of course, the mean pulsar flux is not affected by the scattering, which is an energy-conserving phenomenon).

In this report the parameters of the temporal dispersion function and the scattering cutoff function are derived and applied to the pulsar NP0532. The analysis indicates that the spectrum of the pulsar should be severely distorted by the scattering. The possibility that the low-frequency flux of the pulsar may not be cut off at all (contrary to the apparent pulsation flux) is considered. The angular size, flux, and

position of the "low-frequency compact source" (5-7) in the Crab Nebula, and the excess flux in the overall low-frequency emission of the Crab (8), are good indications that the pulsar may radiate in accordance with the spectrum of its high-frequency pulsation flux down to 10 Mhz.

The geometrical relationship between angular scattering and temporal dispersion is depicted in Fig. 1. Radiation from a point source at a distance L from the observer and scattered through an angle θ (as seen by the observer) at a distance R is delayed relative to unscattered radiation by a time τ :

$$\tau = \alpha R\theta^2/2c \quad (1)$$

where $\alpha = L/(L - R)$ and c is the free-space speed of light; with θ in seconds of arc and L and R in kiloparsecs, $\tau = 1.25 \alpha R\theta^2$ seconds.

From the intensity scintillation of pulsars it is known (2) that the scattering is strong, that is, the root-mean-square phase deviation through the medium is much larger than unity. Thus it is a good approximation to take the distribution function for the two-dimensional angular scattering to be Gaussian regardless of the spatial spectrum of the irregularities of the electron density (9). If the scattering is circularly symmetric, the two-dimensional distribution of scattered flux, defined as $f'(\theta, \phi)$, may then be written as:

$$f'(\theta, \phi) = \exp(-\theta^2/2\theta_0^2)/2\pi\theta_0^2 \quad (2a)$$

where ϕ is the azimuthal angular coordinate and θ_0 is the root-mean-square scattering angle. Thus the fractional flux between θ and $\theta + d\theta$ is

$$f(\theta)d\theta = \int_0^{2\pi} f'(\theta, \phi)\theta d\phi = (\theta/\theta_0^2)\exp(-\theta^2/2\theta_0^2)d\theta \quad (2b)$$

where $f(\theta)$ is the radial flux distribution function. From the change of variables given by Eq. 1 the fractional flux arriving, between time τ and $\tau + d\tau$ after the leading edge of a single pulse has arrived, is:

$$g(\tau)d\tau = (1/\tau_0)\exp(-\tau/\tau_0)d\tau \quad (3)$$

where $g(\tau)$ is the temporal flux distribution function and $\tau_0 = \alpha R\theta_0^2/c$.

If the emitted radiation is a periodic pulse train, then at some time τ after the leading edge of the most recent pulse has arrived, an observer will see not only the contribution $g(\tau)$ of the most recent pulse but also the contributions $g(\tau + T)$ of the previous pulse, $g(\tau + 2T)$ of the pulse which preceded it, and so on. Thus the overall temporal distribution is given by $G(\tau)$:

$$G(\tau) = \sum_{n=0}^{\infty} g(\tau + nT), 0 \leq \tau < T \quad (4)$$

where $g(\tau + nT)$ is the flux contributed by the n th preceding pulse and T is the pulse period. From Eq. 3:

$$G(\tau) = \exp(-\tau/\tau_0) / \{\tau_0[1 - \exp(-T/\tau_0)]\}, \quad 0 \leq \tau < T \quad (5)$$

Thus the observed pulse shape should appear as a sharp rise followed by an exponential decay with time constant τ_0 ; this is precisely what is observed for the pulses of NP0532 at frequencies of ≈ 150 Mhz (10, 11). The scattering parameters may be deduced from the time constant of the pulse decay as:

$$LR\theta_0^2/(L - R) = 0.4 \tau_0 \quad (6)$$

Since θ_0 is proportional to λ^2 [see Ratcliffe (9)], τ_0 is proportional to λ^4 .

Pulse energy that has not decayed by the end of the pulse period will appear only as continuous flux. Thus the fraction of mean pulsar flux which appears as continuous flux is $TG(T)$, and the fraction which appears as pulsation flux is $S_p = 1 - TG(T)$:

$$S_p = 1 - \{y \exp(-y)/[1 - \exp(-y)]\} \quad (7)$$

where $y = T/\tau_0$.

According to Eqs. 5 and 7 the reduction of flux may be estimated by